GRADUATE AERONAUTICAL LABORATORIES

CALIFORNIA INSTITUTE OF TECHNOLOGY

GALCIT Report FM 96-7

INTERACTION OF CHEMISTRY, TURBULENCE, AND SHOCK WAVES IN HYPERVELOCITY FLOW

G. V. Candler*, P. E. Dimotakis, H. G. Hornung, A. Leonard, D. I. Meiron, B. V. McKoy, D. I. Pullin, and B. Sturtevant

*University of Minnesota

Annual Progress Report

Prepared for

AIR FORCE OFFICE OF SCIENTIFIC RESEARCH

110 Duncan Avenue, Suite B115, Bolling AFB DC 20332-0001

Firestone Flight Sciences Laboratory

Guggenheim Aeronautical Laboratory

Karman Laboratory of Fluid Mechanics and Jet Propulsion

Pasadena

INTERACTION OF CHEMISTRY, TURBULENCE AND SHOCK WAVES IN HYPERVELOCITY FLOW

G. V. Candler*, P. E. Dimotakis, H. G. Hornung, A. Leonard,
D. I. Meiron, B. V. McKoy, D. I. Pullin and B. Sturtevant

California Institute of Technology
Pasadena, CA 91125
*University of Minnesota

19 August 1996

Annual Progress Report

Prepared for

AIR FORCE OFFICE OF SCIENTIFIC RESEARCH

110 Duncan Avenue, Suite B115, Bolling AFB DC 20332-0001

AFOSR URI GRANT G - F49620-93-1-0338

INTERACTION OF CHEMISTRY, TURBULENCE AND SHOCK WAVES IN HYPERVELOCITY FLOW

Annual Progress Report
19 August 1996

Principal Investigators:

G. V. Candler, Dept. of Aerospace Engineering and Mechanics
University of Minnesota, Minneapolis, MN 55455

P. E. Dimotakis, H. G. Hornung, A. Leonard, D. I. Meiron
B. V. McKoy, D. I. Pullin, and B. Sturtevant,
California Institute of Technology, Pasadena, CA 91125

Status of Effort

Significant progress was made in the third year of an interdisciplinary experimental, numerical and theoretical program to extend the state of knowledge and understanding of the effects of chemical reactions in hypervelocity flows. The program addressed the key problems in aerothermochemistry that arise from the interaction between the three strongly nonlinear effects: Compressibility; vorticity; and chemistry. Important new results included:

- New data on transition in hypervelocity carbon dioxide flows
- New method of free-piston shock tunnel operation for lower enthalpy
- Accurate new method for computation of self-similar flows
- New experimental data on flap-induced separation at high enthalpy
- Insight into mechanisms active in reacting shear layers from comparison of experiment and computation
- Extensive new data from Rayleigh scattering diagnostics of supersonic shear layer
- Comparison of new experiments and computation of hypervelocity double-wedge flow yielded important differences
- Further first-principles computations of electron collision cross-sections of CO, N_2 and NO
- Good agreement between EFMO computation and experiment of flow over a cone at high incidence
- Extension of LITA diagnostics to high temperature.

Contents

Chapter I: REACTION-RATE CONTROLLED SHEAR FLOW

I.1 TRANSITIONAL AND TURBULENT BOUNDARY LAYERS

Accomplishments, New Findings.

During the first two years of this sub-project, the experimental study of hypervelocity flow over a slender cone yielded the following main results:

1. Air and nitrogen flows up to reservoir specific enthalpies h_0 of 20 MJ/kg could be established in T5. Laminar, transitional and turbulent boundary layers and their demarkation could be visualized by resonantly enhanced interferometry and measured by surface heat flux records. These experiments extended the h_0 range of transition data from the previous highest value of 3 MJ/kg.

2. Evaluating the transition Reynolds number at the reference temperature T^* in the boundary layer, which is logically more meaningful than the edge Reynolds number in the context of transition, correlates the data in a plot agains h_0. This relation shows a massive stabilizing effect of h_0, and a marked difference between air and nitrogen flows.

These results suggested that the appropriate new direction would be to study the flow of a third gas. The main concentration of the work in the reporting period was therefore to repeat the experiments with carbon dioxide flow. CO_2 has a lower dissociation energy than oxygen and nitrogen, as well as a large energy store in easily excited vibration. Any effects from vibration and chemistry should therefore be larger and occur at lower enthalpy. The new experiments benefited from the extension of the data acquisition system to 50 channels that had been installed by one of the industrial users of T5.

The new CO_2 data are plotted together with the air and nitrogen data in Fig. I.1 in the form of transition Reynolds number evaluated at the reference temperature Re^*_{tr} versus h_0. This clearly shows the strong increase of Re^*_{tr} to very much higher values than were reached in air or nitrogen, as well as the expected lower enthalpy at which it appears. It also indicates that the transition Reynolds number does not continue to increase indefinitely with increasing h_0, but levels off at about 6 MJ/kg. A similar leveling off may be expected in the other gases at higher enthalpy.

It is clearly unsatisfactory to show a result in the form of a plot of a dimensionless number versus a dimensional one. Understanding these results demands that the appropriate dimen-

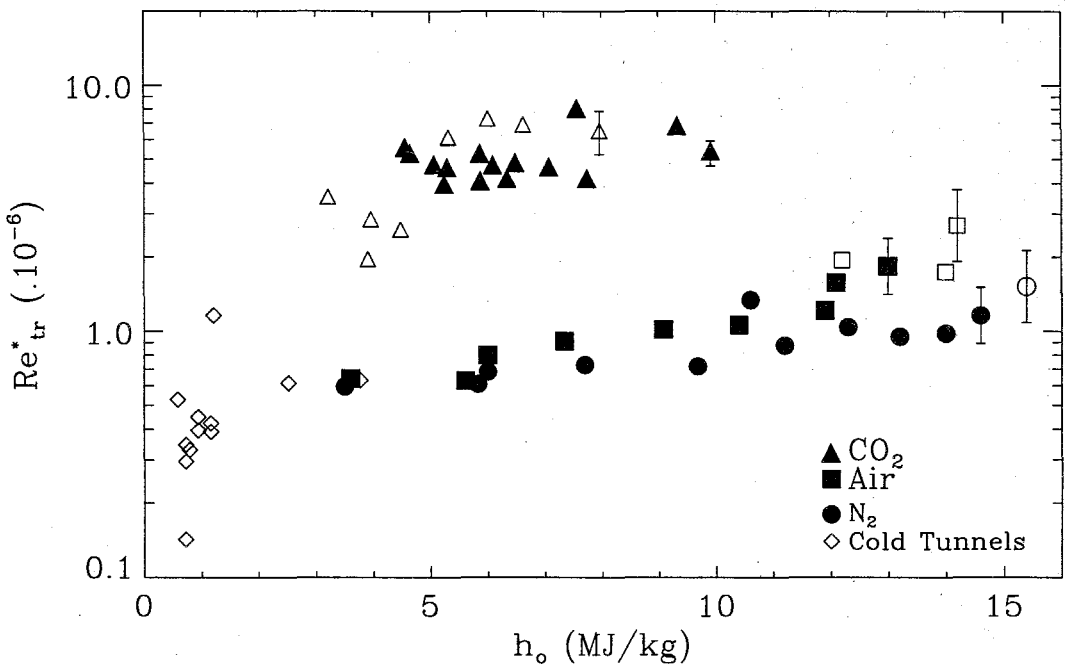

Figure I.1. Correlation of Re^*_{tr} with stagnation enthalpy. Open symbols indicate flows that barely reached transition on the cone. Error bars are estimates of the uncertainty in Re^*_{tr}. Open diamonds clustered to the left show the limited enthalpy range of previous experiments.

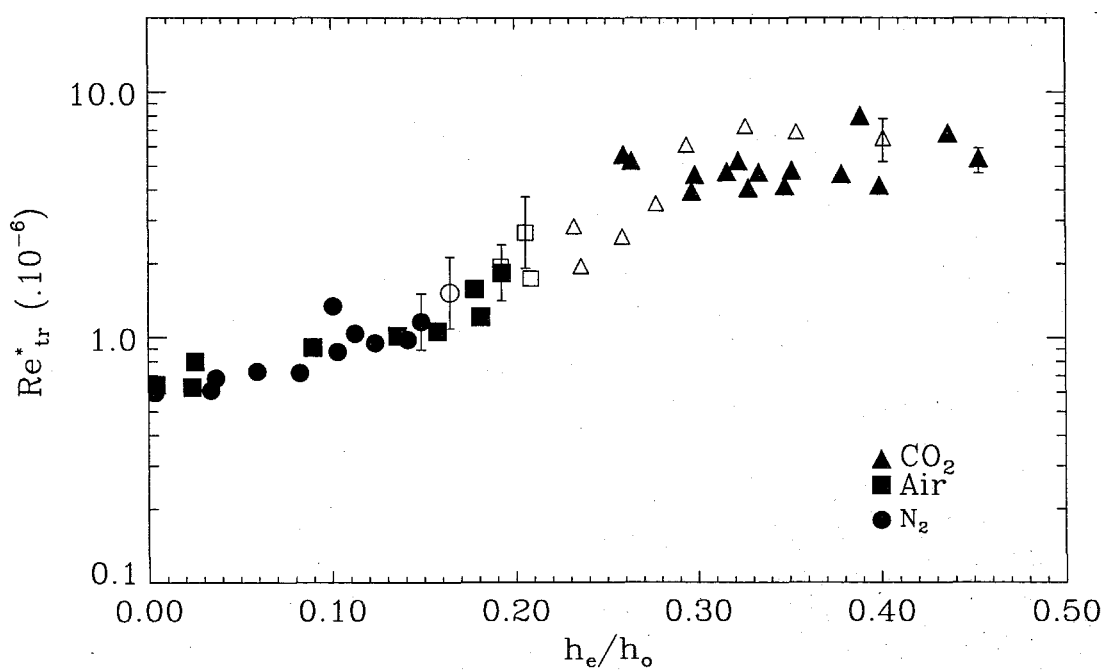

Figure I.2. Replot of the data in Fig. I.1 against h_e/h_0, where h_e is the enthalpy at the edge of the boundary layer.

sionless enthalpy be found. Experimenting with different ways of making h_0 dimensionless led to the form presented in Fig. I.2

Surprisingly, this form of the dimensionless enthalpy correlates the data very well. A mechanism by which the instability of the hypervelocity boundary layer might be damped, such as absorption of acoustic waves by chemical dissipation, appear plausible, but the correlating power of h_e/h_0 is not fully understood.

In parallel with these experiments, extensive computations of the laminar boundary layer with chemical non-equilibrium and surface reactions yielded very good comparison with the air and nitrogen data, but failed to produce the observed values of wall heat flux in the CO_2 results. Reasons for this discrepancy are still being sought.

Personnel Supported

1. Hans G. Hornung, Kelly Johnson Professor of Aeronautics, Director, GALCIT
2. Philippe Adam, Graduate Research Assistant
3. Bahram Valiferdowsi, Associate Engineer

Publications Resulting from Research

1. Germain P. and Hornung H. G. Transition on a slender cone in hypervelocity flow, to appear in *Experiments in Fluids.*
2. Adam P. H. and Hornung H. G. Enthalpy effects on hypervelocity boundary layer transition: Experiments and free-flight data. *AIAA* 97-0764 to be presented at Reno, January 1997.

Interactions/Transitions

1. Application of new operation of T5 (see below), as well as heat-flux sensor technology in tests for Raytheon, Mr. Leo Paradis.
2. Transfer of short-duration hydrogen-injection technology to APRI for tests in T5, Dr. Tom Sobota.

New Discoveries, Inventions, Patents

1. Modified operation of T5 as a piston-compression heated Ludwieg tube for low-enthalpy conditions up to $T_0 = 1100$ K.

Honors/Awards

H. G. Hornung: Foreign Member, Royal Swedish Academy of the Engineering Sciences.

I.2 NONEQUILIBRIUM AND VORTICITY DOWNSTREAM OF BOW SHOCKS

Accomplishments, New Findings.

This subproject has the aim to first use experiment and computation to formulate the theoretical framework of binary scaling of hypervelocity blunt-body flows and its limits, and then to extend the experiments to study the high-vorticity layer downstream of a curved bow shock that is particularly strong in the presence of dissociation. The first part of this task was completed at the end of the second year and is documented in Wen and Hornung (1995).

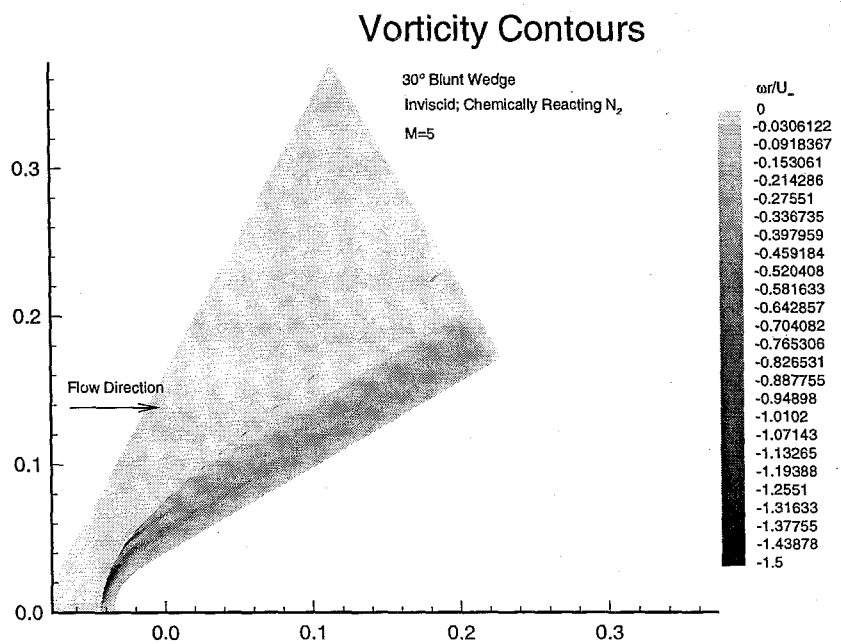

Figure I.3. Vorticity contours in chemically reacting flow of nitrogen over a blunted wedge at 5 km/s and 0.04 kg/m^3.

In order to tackle the second part, the work during the reporting period concentrated on the design of an experiment in which it would be possible to observe effects associated with the high-vorticity layer with techniques such as sodium wire streak visualization (presented in the previous Annual Report: Candler *et al.*, 1995), and interferometry. To this end, an extensive computational study of different configurations was undertaken using the non-equilibrium flow code developed by Candler (1988). The candidate geometries had to generate a high level of vorticity, far from the body, so that the vorticity generated by the shock could be distinguished from that in the boundary layer. The subsequent goal of this investigation is to determine the manner in which this vorticity layer grows and possibly becomes unstable, or interferes with the vorticity produced by the boundary layer.

From the Crocco-Vazsonyi equation it may be shown that in inviscid, homenthalpic, plane flows, the vorticity is proportional to the product of temperature and density. (In isentropic flows, the vorticity is proportional to the density). This was used to narrow down the range of geometries to investigate. For a number of reasons, the best configuration turned out to be a hemispherically blunted wedge. Such a model produces levels of dimensionless vorticity approaching 1 at the shock near the nose, that remain as high as 0.5 far downstream, see Fig. I.3 showing vorticity contours for nitrogen flow at 5 km/s with free-stream density 0.04 kg/m^3.

On the basis of this selection, a model was designed, constructed and equipped with extensive surface heat flux and pressure sensors. These measurements will be complemented by flow visualization using the sodium streak wire, as well as interferometric techniques in a test series due to start in late August 1996.

Personnel Supported

1. Hans G. Hornung, Kelly Johnson professor of aeronautics, GALCIT Director
2. Patrick Lemieux, Graduate Research Assistant
3. Ivett Leyva, Graduate Research Assistant
4. Bahram Valiferdowsi, Associate Engineer

Publications Resulting from Research

1. Wen C.Y. and Hornung H. G. 1995 Nonequilibrium dissociating flow over spheres. *J. Fluid Mech.* **299** 389–405.

References

1. Candler G. V., Dimotakis P. E., Hornung H. G., Leonard A., Meiron D. I., McKoy B. V., Pullin D. I. and Sturtevant B. 1995 Interaction of chemistry, turbulence, and shock waves in hypervelocity flow. Annual Technical Report to AFOSR on URI Grant G-F49620-93-1-0338, GALCIT Report FM 95-3.
2. Candler G. V. 1988 The Computation of Weakly Ionized Hypersonic Flows in Thermo-Chemical Nonequilibrium, Ph.D. thesis, Stanford University.

Interactions/Transitions

1. Invited Presentation at International Conference on the Methods of Aerophysical Research, September 2-6 1996, Novosibirsk (H. G. Hornung and J. J. Quirk)

New Discoveries, Inventions, Patents

None.

Chapter II: SHOCK-VORTICITY INTERACTION

II.1 NONEQUILIBRIUM CHEMISTRY IN SHOCK-VORTEX INTERACTION

Objectives and Status of Research

Work on the computation of steady compressible vortex structures is now almost complete; the objective behind the computation of these flows is to use these special steady solutions as initial conditions for controlled numerical experiments on shock vorticity interactions. To date three types of steady solutions have been successfully computed: arrays of compressible hollow core vortices, arrays of compressible Stuart vortices, and the compressible variant of Hill's spherical vortex. Initial calculations exploring the shock-vortex interaction with these steady solutions are now underway. Extensive computations using a solution technique which allows the computation of similarity solutions for shock-contact interactions both with and without chemistry effects have been carried out. This technique has been used to generate solutions for the regular refraction of a shock by an oblique interface separating two gases. At low density contrasts the effect of chemistry on the circulation is significant. At high density contrast the effect is less pronounced despite significant changes in temperature and density due to dissociation.

The next stage of this work is the completion of the calculations of shock-vortex interaction in the presence and absence of gas dissociation.

II.1.1 Steady compressible vortex structures

Our study of shock vortex interactions requires the computation of steady compressible vortex solutions. These solutions are used as initial conditions to examine the shock-vortex interaction both in the presence and absence of chemistry. The generic mathematical setting for steady compressible vortices is as follows. Consider inviscid compressible flow in a generalized coordinate system (x_1, x_2, x_3) with appropriate scale factors (h_1, h_2, h_3). We consider a steady flow in which the velocity components are nonzero in only the x_1, x_2 directions. Introducing a stream function ψ we can express the velocity $\mathbf{u} = u\mathbf{e_1} + v\mathbf{e_2}$ as

$$h_2 h_3 \rho u = \frac{\partial \psi}{\partial x_2}, \quad h_1 h_3 \rho v = -\frac{\partial \psi}{\partial x_1}, \tag{1}$$

where ρ is the density of the flow. For steady compressible flow it is easy to show that

$$(\mathbf{u} \cdot \nabla) S = 0 \;\Rightarrow\; S = S(\psi) \tag{2}$$

$$(\mathbf{u} \cdot \nabla) H = 0 \;\Rightarrow\; H = H(\psi) \tag{3}$$

where S is the entropy, $H = 1/2(u^2+v^2)$ is the total enthalpy, and h is the specific enthalpy. Using Crocco's theorem $\nabla H = T\nabla S + \mathbf{u} \times \omega$ in conjunction with the equations above it follows that

$$\frac{\omega}{h_3 \rho} = T\frac{\partial S}{\partial \psi} - \frac{\partial H}{\partial \psi}. \tag{4}$$

We have formulated both the homentropic ($S = const$) and the homenthalpic ($H = const$) cases which are respectively

$$\frac{\omega}{h_3 \rho} = -\frac{\partial H}{\partial \psi} \equiv V(\psi), \qquad \frac{\omega}{h_3 \rho T} = -\frac{\partial S}{\partial \psi} \equiv W(\psi), \tag{5}$$

We have only considered the homentropic case in our work to date although the homoenthalpic case is also of physical interest. A closed system of equations for $\psi(x_1, x_2)$ and $\rho(x_1, x_2)$ can be obtained by introducing the equations of state for a calorically perfect gas in homentropic flow, and making use of the energy equation, together with the relation $H = H_0 - \int_0^{\psi} V(\psi')d\psi'$. After scaling with appropriate reference variables we obtained the nonlinear system

$$-\frac{1}{h_1 h_2 h_3 \rho}\left[\frac{\partial}{\partial x_1}\left(\frac{h_2}{h_1 h_3 \rho}\frac{\partial \psi}{\partial x_1}\right) + \frac{\partial}{\partial x_2}\left(\frac{h_1}{h_2 h_3 \rho}\frac{\partial \psi}{\partial x_2}\right)\right] = V(\psi), \tag{6}$$

$$\frac{M_\infty^2}{2}\left[\frac{1}{h_1^2}\left(\frac{\partial \psi}{\partial x_1}\right)^2 + \frac{1}{h_2^2}\left(\frac{\partial \psi}{\partial x_2}\right)^2\right] + \frac{\rho^{\gamma+1}}{\gamma - 1} = \rho^2 h_3^2 H(\psi). \tag{7}$$

where M_∞ is the Mach number (measured relative to conditions at infinity). These equations have now been solved for three different cases corresponding to different boundary conditions and a different choice of $V(\psi)$:

1. compressible hollow core vortices. This has been described in our previous report and is now published (Ardalan *et al* 1995). An interesting aspect of these solutions is the presence of shock-free transonic solutions.

2. compressible Stuart vortices. These are compressible analogues of the classical incompressible solution first discussed by Stuart. The Stuart vortices can be continued to finite M_∞ using $V(\psi) = \exp(-2\psi)$. These solutions can be used as a model of the non-linear phase of a compressible shear layer. This work is is discussed in the Ph.D. thesis of Kayvan Ardalan (1995).

3. compressible Hill's Spherical Vortex. In preliminary work this problem has been studied with Prof. D. W. Moore of Imperial College, London. Here we choose (x_2, x_2, x_3) as spherical coordinates (r, θ, ϕ) where r is the radius and θ is the polar angle. The continuation of the incompressible solution along a branch representing homentropic flow at finite M_∞ was made with the choice $V(\psi) = -15/2, \quad \psi < 0, V(\psi) = 0, \quad \psi > 0$. The flow is rotational for $r < 1$ and irrotational for $r > 1$. With $(h_1, h_2, h_3) = (1, r, r\sin\theta)$, we have two PDE's for ψ and ρ. The vortex boundary corresponds to $\psi = 0$ which must be determined as part of the solution. We solved the nonlinear

PDE's using finite differences. Two preliminary results are noted. First, the vortex boundary which is a sphere when $M = 0$ becomes a prolate spheroid elongated along the direction of the free stream. Second, the flow becomes sonic at the origin at $M_\infty = 0.58$ approximately. Continuation beyond the locally sonic state is currently under study.

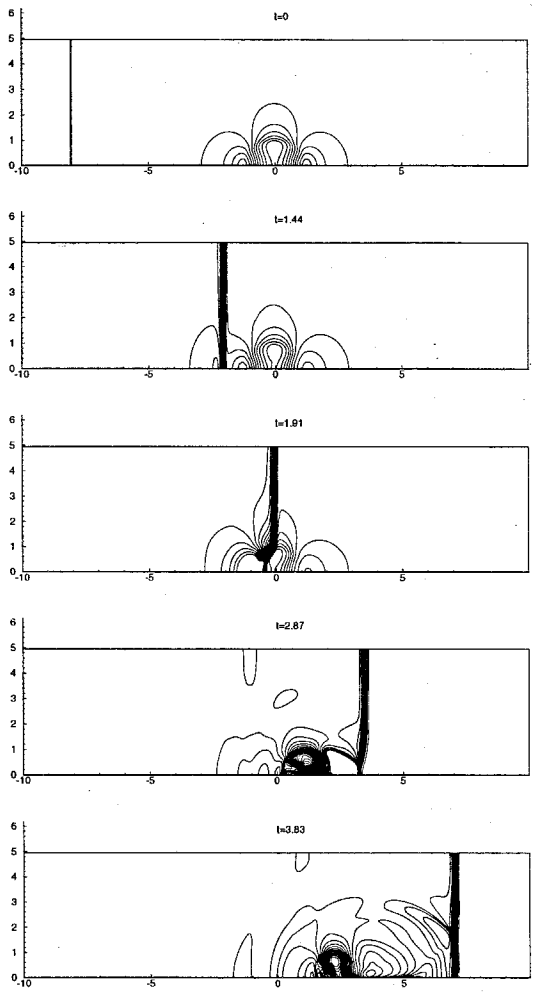

Figure II.1. Density images showing the impingement of a shock wave on a stationary compressible Hill spherical vortex. The shock pressure-ratio is 2.5 and the vortex Mach number is $M_\infty = 0.5$.

II.1.2 Shock-Vortex Interaction

We have performed calculations of the interaction of a Mach 1.5 shock with a compressible Hill's spherical vortex. Fig. II.1 we show density contours for this interaction. In future work we will perform a thorough investigation of the parameter space at high resolution to study the dynamics of the shock-vortex interaction using the steady solutions derived above.

In addition the effects of dissociation will also be investigated using the EFM technique for numerical simulation discussed in our previous report.

II.1.3 Self-similar roll up of a vortex layer in a density stratified compressible fluid

We have developed an iterative technique for computation of conically self-similar solutions of the two-dimensional unsteady Euler equations (Samtaney & Pullin, 1996, Samtaney 1996). The idea is to search for solutions of the to the Euler equations of the form

$$U(x,y,t) = (\rho(\xi,\eta), u(\xi,\eta), v(\xi,\eta), E(\xi,\eta)), \qquad \xi = x/t \qquad \eta = y/t. \tag{8}$$

Using this similarity transformation on the Euler equations leads to the nonlinear system

$$2\tilde{U} + \tilde{F}_\xi + \tilde{G}_\eta = 0, \tag{9}$$

where

$$\tilde{F} = \{\rho(u-\xi), \rho u(u-\xi) + p, \rho v(u-\xi), E(u-\xi) + pu\}^T, \tag{10}$$

$$\tilde{G} = \{\rho(v-\eta), \rho u(v-\eta), \rho v(v-\eta) + p, E(v-\eta) + pv\}^T. \tag{11}$$

This approach can be applied to a fairly wide variety of two dimensional flows which include the diffraction of a plane shock wave by an oblique interface. We solved the above boundary value problem directly by an approximate Newton method. The numerical method is based on direct evaluation and iterative inversion of the Jacobian for both the implicit Godunov and implicit Equilibrium Flux methods. A striking feature of the solutions is that flow discontinuities are resolved much more sharply. In addition the technique computes reliably the self-similar roll-up of the contact discontinuity which becomes a vortex sheet after the shock has interacted with the interface. Shown in Fig. II.2 is the refraction of a Mach 2.02 shock wave at a gaseous interface separating gases of density $\rho_1 = 1$, $\rho_2 = 3$ inclined at an angle of $\alpha = 60°$ to the plane of the shock. The interface is initially in thermal and mechanical equilibrium. The spiral associated with the rollup of the vortex sheet is clearly seen and in contrast to solutions obtained using the initial value problem, it is completely reproducible without the artifacts normally seen in initial value calculations. Further, the similarity calculations exihibit convergence with respect to grid refinement unlike initial-value calculations.

We have extended these ideas and investigated the self-similar interaction of a strong shock including the effects of equilibrium dissociation chemistry. We have observed that the transition from regular to irregular refraction is slightly delayed by equilibrium chemistry effects in most cases.

Publications Resulting from Research 1995-96

Ardalan,K., Meiron, D.I.& Pullin, D.I., 1995, "Steady compressible vortex flows- the hollow-core vortex array". *J. Fluid Mech.*, **301**, pp1-17.

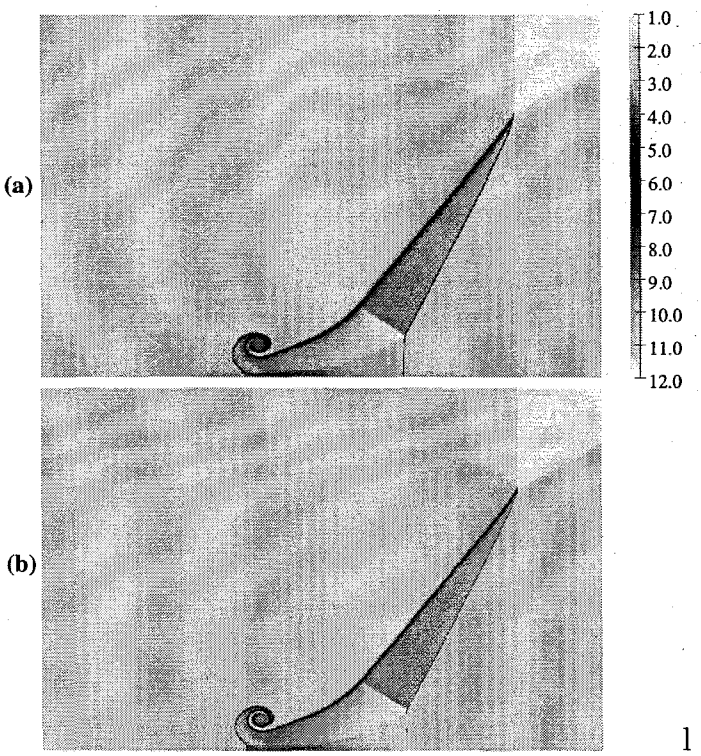

Figure II.2. Density images for the self-similar solution for a shock wave impinging on a density interface. Grid sizes: (A) 768 × 392, (B) 1536 × 768

Samtaney, R. & Pullin, D. I. 1996, "On similarity and initial-value solutions of the compressible Euler Equations". Accepted by *Physics of Fluids.* In press

Samtaney, R. 1996, "A method for constructing similarity solutions to the time-dependent multi-dimensional Euler equations.". Sub judice, *J. Comp. Phys.*

Samtaney, R., & Meiron, D. I. 1996. "Hypervelocity Richtmyer-Meshkov Instability". Sub judice, *Phys. Fluids*

Personnel Supported

1. Daniel I. Meiron, Professor of Applied Mathematics
2. Dale I. Pullin, Professor of Aeronautics
3. Dr. Ravi Samtaney, Senior Research Associate

Interactions/Transitions

(a) Participations/presentations at meetings etc.

- Samtaney, R. & Pullin, D. I., "On self-similar solutions of the compressible Euler Equations". *Presented at the APS meeting, November 1995, Irvine CA.*

- Meiron, D., Meloon. M. & Samtaney, R. , "Models for vorticity generation in Richtmeyer-Meshkov instability". *Presented at the SIAM annual meeing, October 1995.*

(b) Consultative and advisory functions etc.

None.

(c) Transitions

None.

New discoveries, inventions, patents

None.

Honors/Awards etc. None.

II.2 SHOCK WAVE INTERACTIONS IN HYPERVELOCITY FLOW

Accomplishments/New Findings

A study of real-gas effects on stagnation-point heat transfer near shock impingement on a bluff body in hypervelocity flow (the so-called shock-on-shock problem) has been completed and reported in the last Progress Report. The focus of this experimental investigation has now moved to a study of the effects of dissociation and recombination on maximum heat transfer and boundary layer stability in hypervelocity flow over a compression ramp. The flow over a flat plate[1] with a deflected flap is an important Problem in reentry aerodynamics. This point was graphically impressed on the hypersonics community during the first STS reentry, when it was discovered that the flap effectiveness was less than had been predicted based on the understanding of that day. The effects of relaxation processes on surface pressure and heat transfer at reentry conditions remain to this day to be experimentally documented.

As with the shock-on-shock problem, flow over a flat plate with a deflected flap involves the impingement of a shear layer on the body, with consequent high heating. This configuration was studied extensively in cold-flow wind tunnels in the past. In the case of the shock-on-shock problem, we have found that a subtle balance of shock waves in the shock layer

[1]The plate may or may not be at angle of attack.

near the shear layer reduces the influence of thermochemistry on the flow, so anticipated enhanced heating at shock impingement does not occur. This balance is not expected in the flow over a compression ramp. On the other hand, we expect that pressures and heat flux may be substantially altered at large plate and/or flap incidences, when dissociation behind the resulting strong shock waves significantly alters the flow density.

Two configurations which are likely to produce measurable real gas effects are being treated. One is the flat plate at zero incidence with moderately high flap deflection (greater than 30°). If the reattachment shock is strong enough to cause significant dissociation, an increase of peak heat transfer on the flap may be observable at high enthalpy. The second configuration, a flat plate at incidence with varying flap deflection, is more applicable to real flows found on aerospace vehicles. For example, the shuttle orbiter often flies at 35° angle of attack during reentry. At high enthalpy, the leading edge shock can cause significant dissociation, which can not only affect the separation region because of changes of the boundary layer thickness but also by changes in the local Mach and Reynolds numbers; the separation length scales with increasing Re and decreasing M, and thus the flap angle at which flow separation first occurs (incipient separation) scales in the opposite directions. Parameters being examined in this study include pressure and heat transfer distributions, incipient separation angle, separation length and three-dimensional boundary layer structure downstream of reattachment.

During the present reporting period preliminary experiments have been carried out on a modified existing model and, based on those results, a 2-dimensional model specially designed for this study has been fabricated. Figure II.3 shows a top view and side view of the model. The model consists of a four-inch chord, eight-inch span forward plate with replaceable sharp

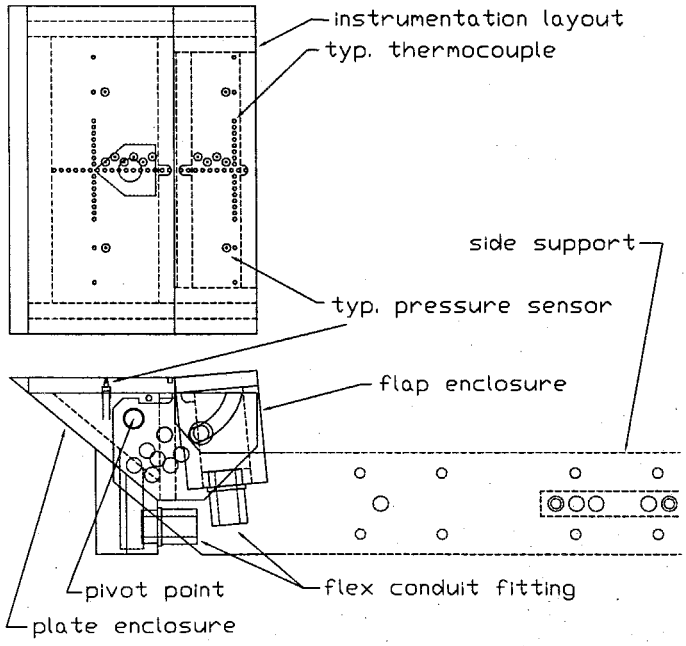

Figure II.3.

leading edge and a full-span, two-inch chord trailing flap. This sizing was selected to give an

aspect ratio greater than unity while allowing visualization (by shadowgraphy) of the entire flow field in T5's eight-inch diameter optical access windows. The forward plate and flap have separate enclosures for instrumentation and cabling. The forward plate enclosure is sloped 40° in front for attached flow at the zero-degree angle of attack position. The rear wall of the plate enclosure and the front wall of the flap enclosure are keyed for a series of wedges to be installed between them, each wedge producing a different flap angle with respect to the front plate (from 5° to 40°) and also ensuring proper alignment along the length of the hinge line. The side walls of the front plate enclosure extend back alongside the flap enclosure, where bolts hold the flap enclosure in place (note that moment loads about the hinge line during a test are taken up by the above-mentioned wedges, not these bolts). The entire model pivots about a spanwise axis through the front plate enclosure to vary the angle of attack for the front plate with respect to the free stream flow. The model is locked in place at each of five different angles (from 0° to 40°) by bolts through the side supports and by a series of blocks inserted underneath the side overhangs of the front plate and keyed to the side supports.

The instrumentation includes 67 thermocouples, although the current T5 data acquisition system can only simultaneously record 52 channels of model instrumentation. Under normal operation, only 35–39 of the thermocouples will be used, to provide full streamwise data plus data from several spanwise thermocouples to check three-dimensionality of the heat transfer far away from the centerline. When detailed information is desired on the spanwiase variation of heat transfer, all of the spanwise arrayed thermocouples can be recorded in place of the pressure sensors and some of the streamwise thermocouples. Forty of these thermocouples have been assembled in-house using existing parts left over from previous work in T5; the remaining 27 spanwise locations on the model are fitted with new transducers. Pressure measurements are made with 14 miniature PCB105B12 gauges.

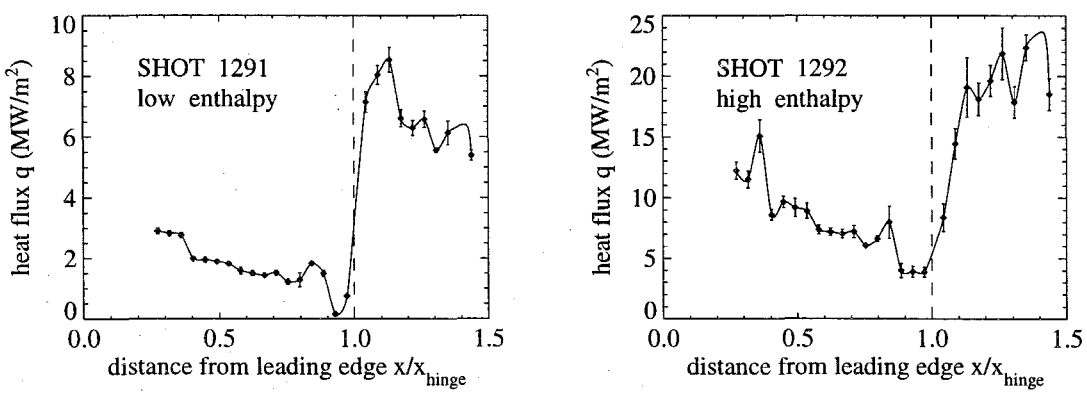

Figure II.4.

Figure II.4 shows some recent heat flux measurements from experiments in T5 using the model described above. Error bars indicate unsteadiness in the heat flux, the solid line is a spline fit to aid in visualization, and the dashed line is the hinge location. The sudden drop in heat flux upstream of the hinge line indicates a region of separated flow due to the 15° flap deflection. The upstream extent of this region is clearly smaller for the low enthalpy case

in shot 1291. The run conditions for these two shots were designed, using nitrogen test gas and a conical nozzle of variable area ratio, to show the effect of dissociation at the boundary layer edge for constant viscous interaction parameter $\bar{\chi} = M_e^3/\sqrt{Re_x}$, which defines flat plate boundary layer growth in cold hypesonic flow. The forward plate is at angle of attack (35° in shot 1291 and 40° in shot 1292) such that, for inviscid frozen flow on the plate, $\bar{\chi}$ at $x = x_{hinge}$ is approximately 0.0275 in both cases. The difference in reservoir enthalpy, however, produces an atomic mass fraction at the boundary layer edge (for frozen flow this is equal to the mass fraction in the nozzle free stream) of $\alpha =$ for shot 1291 and $\alpha = 0.13$ for shot 1292. Since separation length (here measured upstream from the hinge line) scales with boundary layer thickness, the longer upstream extent of separation in shot 1292 may arise from an increased boundary layer thickness due to mass diffusion between the partially dissociated gas at the boundary layer edge and the recombined gas at the cold wall.

Personnel Supported

1. B. Sturtevant, Professor of Aeronautics.
2. Jean-Paul Davis, Graduate Student.

Publications

Sanderson, S.R. and Sturtevant, B., 1996, Shock-interference heating in hypervelocity flow, in *Shock Waves*, Proc. 20th Symp. on Shock Waves, World Scientific, Singapore, p. 209.

Interactions

1. Organized and participated in the 20th Symposium on Shock Waves, Pasadena, CA, July, 1995.
2. Collaboration with ESA-ESTEC on shock-wave boundary-layer interaction in hypervelocity flow. Ref: GALCIT Reports FM 94-4 and FM 96-2.

Inventions

1. None.

Honors/Awards

1. B. Sturtevant: Fellow, American Physical Society.
2. S. Sanderson: Ballhaus Prize, GALCIT Ph. D. Thesis, 1995, shared.

Chapter III: SUPERSONIC SHEAR-FLOW MIXING AND COMBUSTION

Accomplishments / New Findings

Further studies of turbulent mixing and combustion at high-compressibility conditions are in progress. Specifically, a high-Mach-number model is under design for use in the existing Supersonic Shear Layer, (S^3L) Facility. The model, shown schematically in Fig. III.1, will use a (supersonic) expansion turn to accelerate the top freestream flow from $M_0 \approx 1.5$ to $M_1 \approx 3.5$. The secondary, low-speed flow will be introduced through an array of small holes in the post-expansion guidewall. A preliminary design employed commercially-available, sintered-metal porous plate. In a series of feasibility tests, however, the plate porosity and resulting flow were found to be highly non-uniform, rendering it unsuitable. Experiments are currently underway to characterize the stability of an array of jets, *i. e.*, flow through closely-spaced holes, in a crossflow.

Utilizing the capabilities of the existing facility, H_2+NO will be introduced as reactants to the top, supersonic stream, and F_2 to the bottom, low-speed (transpiration) stream. We intend to investigate the region of moderate-to-high heat release in this flow and, in particular, the drag-reducing displacement effect of combustion-induced dilatation.

As part of a collaborative effort between USC and Caltech, cofunded by AFOSR Grant No. F49620–94–1–0353, numerical simulations of strained flames of the $H_2 + NO/F_2$ system were performed corresponding to strain rates encountered in the chemically-reacting supersonic shear layer flows we have been investigating in the recent past (Hall *et al.* 1991). A comparison of the result of these simulations with the experimentally-observed chemical-product formation, in the fast kinetic (high-Damköhler-number) regime of these experiments, indicates that the preponderant fraction of chemical production and heat release occurs with

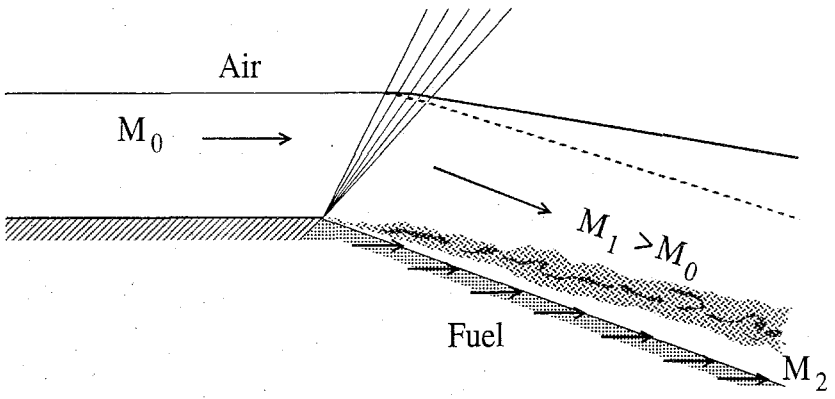

Figure III.1. Schematic of supersonic expansion turn model. Dashed streamline: no heat release; solid streamline: displaced by heat release.

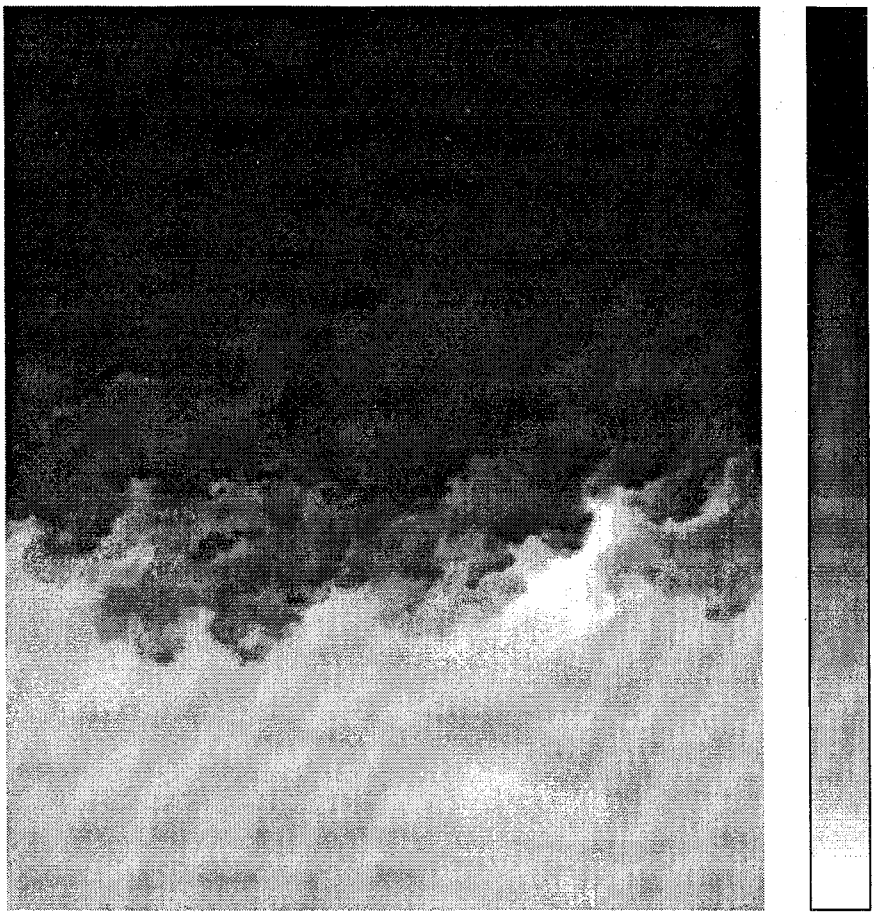

Figure III.2. Molecular planar laser-Rayleigh scattering image of a $M_1 = 1.5$ [He] over $M_2 = 0.3$ [C_2H_4] supersonic mixing-layer.

the reactants in a premixed, rather than diffusion-layer, mode. This may be regarded as a general result for high-strain-rate flows and was recently reported at the 26th International Combustion Symposium (Egolfopoulos *et al.* 1996).

The scalar mixing field in supersonic mixing layers, at high-speed freestream Mach numbers in the range, $0.6 \leq M_1 \leq 1.55$, corresponding to convective Mach numbers in the range, $0.15 \leq M_c \leq 0.95$, where $M_c \equiv (U_1 - U_2)/(a_1 + a_2)$, was studied using molecular laser-Rayleigh scattering images in a streamwise, mid-span plane of the flow. Individual realizations show that, even as compressibility is increased, the entrainment and mixing processes occur through the action of large-scale structures that, however, are less organized than those encountered in lower compressibility shear layers. As illustrated in Fig. III.2, a convecting wave system is present in the low-speed freestream for the $M_c = 0.95$ case. This wave system has been documented in previous schlieren data (Hall *et al.* 1993) and is caused by large-scale structures that are convecting supersonically with respect to the low-speed (lab-frame subsonic) freestream. This part of the effort is cofunded by AFOSR Grant No. F49620–94–1–0353.

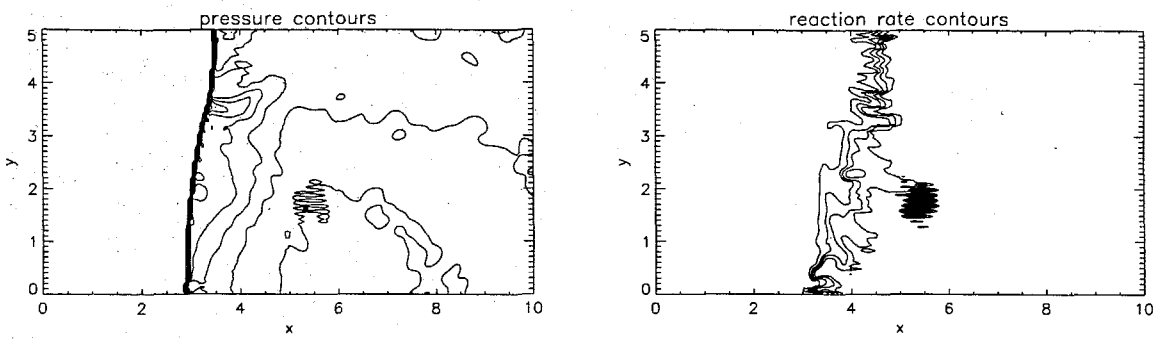

Figure III.3. Unstable detonation propagating through a channel. Pressure and reaction-rate contours at $t = 8.0$. The resolution is 20 points per half-reaction length.

As part of our work on computing compressible, chemically-reacting flows, we have developed a new algorithm that integrates all the terms of the governing equations simultaneously. No flux-splitting, or other "fixes", usually employed, are needed. The algorithm is compatible, and has been used, with adaptive gridding algorithms, as part of the *Amrita* package, developed by James Quirk (Quirk 1996).

This multidimensional, unsplit scheme is an extension of the original, one-dimensinal implementation (Papalexandris *et al.* 1996) and is currently being used to study, numerically, 2-D detonation phenomena. As an example, computed contour levels of the pressure and the reaction-rate variable of a detonation front propagating in a channel are depicted in Fig. III.3. A ZND profile for an overdrive factor of $f = 1.60$ was used as the initial condition. The shock wave was initially located at $x = 4.0$. The material upstream of the front is unreacted. The top and bottom boundaries are reflecting walls, while the left and right boundaries are inflow and outflow boundaries, respectively. The results presented are taken at $t = 8.0$. Other interesting phenomena, including the stability of oblique detonations, are currently been investigated with the present scheme.

References

Egolfopoulos, F. N., Dimotakis, P. E., and Bond, C. L., 1996 On Strained Flames with Hypergolic Reactants: The $H_2/NO/F_2$ System in High-Speed, Supersonic and Subsonic Mixing-Layer Combustion, *Twenty-Sixth Symposium (International) on Combustion (Naples, Italy), The Combustion Institute, Pittsburgh*, Paper 310.

Hall, J. L., Dimotakis, P. E., and Rosemann, H. 1991 Some measurements of molecular mixing in compressible turbulent mixing layers, *AIAA* 22$^{\text{nd}}$ *Fluid Dynamics, Plasma Dynamics and Lasers Conference* (Honolulu, 24–26 June 1991), Paper 91–1719.

Hall, J. L., Dimotakis, P. E., and Rosemann, H. 1993 Experiments in non-reacting compressible shear layers, *AIAA J.* **31**(12), 2247–2254.

Papalexandris, M. V., Leonard, A., and Dimotakis, P. E. 1996 Unsplit Schemes for Hyperbolic Conservation Laws with Source Terms in One Space Dimension, California Institute of Technology, GALCIT Report FM96–1.

Quirk, J. J. 1996 An Introduction to AMRITA, California Institute of Technology, Ae240 class notes.

Personnel Supported

1. Dahl, E. E., Member of the Technical Staff, Aeronautics
2. Dimotakis, P.E., Professor, Aeronautics and Applied Physics (Co-PI)
3. Fourguette, D. C., Senior Research Fellow, Aeronautics
4. Gornowitz, G. G., Graduate Research Assistant, Aeronautics
5. Lang, D. B., Research Engineer, Aeronautics
6. Leonard, A., Professor, Aeronautics
7. Melvin, J. D., Member of the Technical Staff, Eng. and Applied Sc.
8. Papalexandris, M. V., Graduate Research Assistant, Aeronautics
9. Quirk, J. J., Senior Research Fellow, Aeronautics
10. Rodriguez, A. M., Administrative Assistant
11. Slessor, M. D., Graduate Research Assistant, Aeronautics
12. Svitek, P., Staff Engineer

Collaborations (not URI supported)

1. Collins, A., JPL (digital imaging)
2. Egolfopoulos, F., Assistant Professor. Mech. Eng., USC
3. Elliot, T., JPL (digital imaging)
4. Janesick, J. R., PixelVision Corporation (digital imaging)

Publications

- Egolfopoulos, F. N., Dimotakis, P. E., and Bond, C. L., "On strained flames with hyperbolic reactants: The $H_2/NO/F_2$ system in high-speed, supersonic and subsonic mixing-layer combustion," 26th Int. Symposium on Combustion, 28 July - 2 August 1996 (Naples, Italy), Paper 310.
- Papalexandris, M. V., Leonard, A., Dimotakis, P. E., "Unsplit schemes for hyperbolic conservation laws with source terms in one space dimension," J. Comp. Physics (submitted).

Interactions/Transitions

a. Participation/Presentations

1. Dimotakis, P., Fourguette, D. C., Gornowicz, G. G., Slessor, M. D.: 48th APS/DFD meeting (Irvine, CA), 19-21 November 1995 (3 presentations of work sponsored under this Grant).

2. Dimotakis, P.: AFOSR NO vitiation workshop (hypersonic testing facilities), 17 Jan 1996 (Reno, NV).

3. Dimotakis, P.: AFOSR/NASA Scramjet Combustion Workshop (Newport News, VA), 14–16 May 1996.

4. Dimotakis, P., Egolfopoulos, F. N.: 26th Int. Symposium on Combustion, 28 Jul - 2 Aug 1996 (Naples, Italy), coauthor on paper presented w. F. Egolfopoulos (see above).

b. Consultative and advisory functions

- Dimotakis, P. E.: Lawrence Livermore National Laboratories, consulting on compressible turbulence and inertial-confinement fusion.

c. Transitions

None

New Discoveries/Inventions

None

Honors/Awards

Dimotakis, P. E.

- John K. Northrop Chair, Aeronautics, Caltech (Feb 1995)
- Associate Fellow, AIAA (June 1989)
- Fellow, Am. Phys. Society (November 1980)

Chapter IV: CHEMISTRY IN NONUNIFORM FLOW

IV.1 DISSOCIATION RATES WITH VIBRATIONAL NONEQUILIBRIUM

4. Accomplishments / New Findings

One of the primary uncertainties in the modeling of hypersonic reacting flows is how the vibrational state of a molecule affects its dissociation rate. Therefore, the main objective of this research is to test chemical reaction rate models in the presence vibrational nonequilibrium. Our initial work showed that the flow of nitrogen over spheres at typical T5 conditions is not very sensitive to the choice of several popular vibration-dissociation coupling models. Therefore, we used computational fluid dynamics to design a new experiment that shows strong sensitivity to the coupling model. We found several geometries and flow conditions that are good candidates, and they have been tested in the free-piston shock tunnel, T5, at Caltech. Currently, the data are being analyzed. We expect that this experiment will provide the first data that can be used for the direct validation of vibration-dissociation coupling models, and it will provide new insight into how the vibrational state affects the dissociation rate.

The experimental configurations are either double-wedge or double-cone geometries; the first cone or wedge causes an attached shock wave to form which interacts with the detached shock from the second wedge or cone. This creates a complicated flow field that is very sensitive to the vibration-dissociation coupling model. Typically, the popular Park $\sqrt{TT_v}$ coupling model produces a flow field with a smaller separation zone than the Marrone and Treanor CVDV model. The difference in the separation zone causes a large change in the surface pressure distribution and in the convective heating rate distribution.

Two sets of experiments were performed. The first used a finite-length double-wedge geometry instrumented with pressure and heat transfer gauges, and the second used a series of double cones. The nominal test conditions were pure nitrogen at a total enthalpy of 26.1 MJ/kg and a stagnation pressure of 36.7 MPa. In both cases Mach-Zehnder interferograms were made. The analysis of the experimental data is underway. To date, we have made three-dimensional computational fluid dynamics simulations of the flow over the double wedges at the experimental conditions. At this point, there is poor agreement between the experiments and the computational results; a typical comparison is shown in Fig. IV.1 and Fig. IV.2. We see that the computation significantly underpredicts the size of the separation zone and the details of the shock-shock interaction. The reason for this discrepancy is presently unknown.

During the design of the double-wedge experiments, we discovered some interesting flow features and what appears to be a new shock-shock interaction. For example, the Mach

6.9 flow of a perfect gas over a 15°–58° double-wedge creates a shock-shock interaction that is similar to, but different than, a Type IV interaction. As seen in Fig. 3, the shock that is transmitted from the triple point undergoes a regular reflection from the first wedge surface, creating a supersonic flow along the surface of the body. This flow is similar to an underexpanded jet, making it undergo alternating expansions and recompressions. A series of experiments has been designed for the Mach 8 blow-down wind tunnel at Princeton University; preliminary testing has started, and the final runs will be complete by the end of the summer.

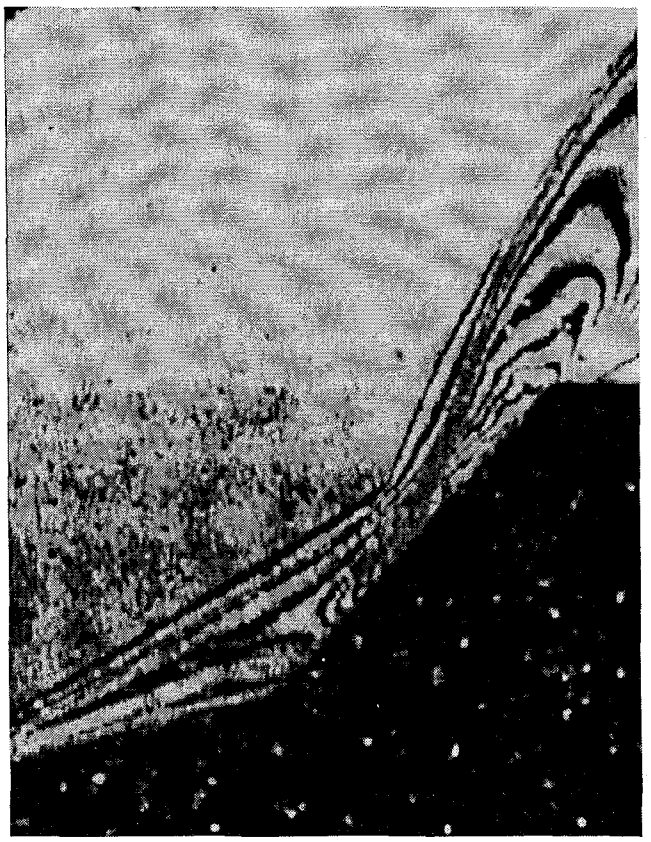

Figure IV.1. Experimental interferogram for T5 Shot 1049 ($\rho_\infty = 0.0078\,\mathrm{kg/m^3}$, $T_\infty = 1888\,\mathrm{K}$, $u_\infty = 6110\,\mathrm{m/s}$, base height is 2 inches (5.08 cm)).

5. Personnel Supported

Graham V. Candler, Associate Professor of Aerospace Engineering and Mechanics, University of Minnesota.

Joseph Olejniczak, Graduate Research Assistant, Department of Aerospace Engineering and Mechanics, University of Minnesota.

6. Publications Resulting from Research: Oct. 1995 – Oct. 1996

Olejniczak, J., G.V. Candler, and M.J. Wright, "Numerical Study of Shock Interactions on

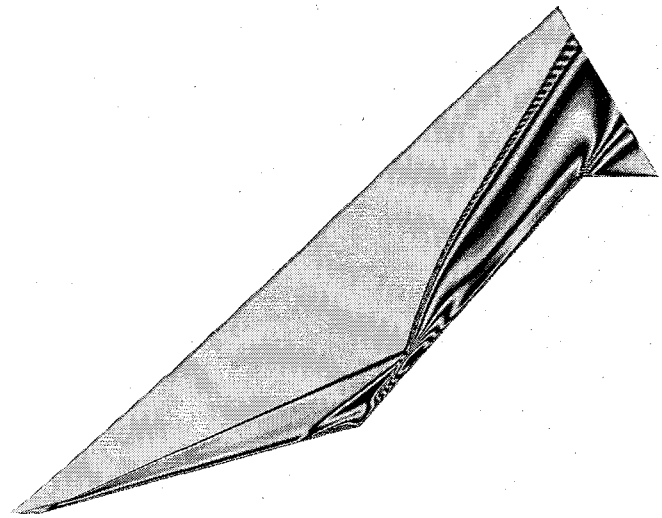

Figure IV.2. Computational interferogram for T5 Shot 1049 at the same flow conditions as Fig. IV.1.

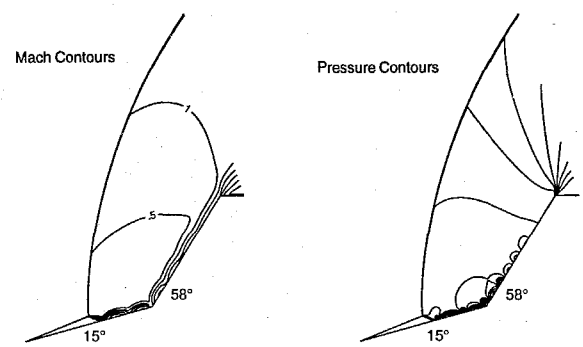

Figure IV.3. Mach number and pressure contours of the new shock interaction. The flow is inviscid with shock interaction. The flow is inviscid with $M_\infty = 6.9$ and $\gamma = 1.4$; computation performed on a 512×512 grid.

Double-Wedge Geometries," extended abstract submitted for presentation at the 34th AIAA Aerospace Sciences Meeting, Jan. 1996.

Candler, G.V., J. Olejniczak, and B. Harrold, "Detailed Simulation of Nitrogen Dissociation in Stagnation Regions," *AIAA Paper No. 96-2025,* June 1996.

Olejniczak, J., and G.V. Candler, "High Enthalpy Double-Wedge Experiments," *AIAA Paper No. 96-2238,* June 1996.

Candler, G.V., D. Bose, and J. Olejniczak, "Interfacing Nonequilibrium Models with

Computational Fluid Dynamics Methods," *Molecular Physics and Hypersonic Flows,* Ed. M. Capitelli, Kluwer Academic Publishers, Dordrecht, Netherlands, 1996, pp. 625-644.

Olejniczak, J., M.J. Wright, and G.V. Candler, "Classification of Shock Interactions on Double-Wedge Geometries," submitted to the *Journal of Fluid Mechanics,* Aug. 1996.

Wright, M.J., J. Olejniczak, and G.V. Candler "Numerical and Experimental Investigation of Double-Cone Shock Interactions," extended abstract submitted for presentation at the *35th AIAA Aerospace Sciences Meeting,* Jan. 1997.

7. Interactions/Transitions

Presentation of papers at:

34th AIAA Aerospace Sciences Meeting, Reno, NV, Jan. 1996.

27th AIAA Fluid Dynamics Conference, New Orleans, LA, June 1996.

19th AIAA Advanced Measurement and Ground Testing Technology Conference, New Orleans, LA, June 1996.

31st AIAA Thermophysics Conference, New Orleans, LA, June 1996.

Plasma Based Hypersonic Drag Reduction Workshop, Wright-Patterson AFB, OH, May 1996.

ARO/BMDO Missile Signatures Meeting, Moffett Field, CA, April 1996.

NASA Ames Research Center, Moffett Field, CA, April 1996.

AHPCRC Infrastructure Support Scientists Workshop, Aberdeen, MD, Feb. 1996.

AHPCRC Seminar, Minneapolis, MN, April 1996.

Consultative Functions:

G.V. Candler presented a talk at the Plasma-Based Hypersonic Drag Reduction Workshop, Wright-Patterson AFB, OH, May 1996. Wrote comments concerning issues associated with methods for plasma-based drag reduction and computational methods for the simulation of ionized hypersonic flows.

Transitions: None.

8. New Discoveries

The computational work used to design the experimental configurations for vibration-dissociation model testing resulted in the discovery of a new shock-shock interaction that occurs in hypersonic flows. This interaction is similar to the Type IV interaction of Edney, and results in very large surface pressure and heat transfer variations on the body surface. This effect could be important in the design of control surfaces for hypersonic vehicles.

9. Honors/Awards: None.

IV.2 ELECTRON-DRIVEN REACTIONS IN HYPERSONIC FLOW

Background and Objective

Electrons resulting from ionization due to bow shock heating play an important role in determining the chemical and physical properties of hypersonic flows. Due to non-equilibrium overshoots, electron temperatures can be as high as 10,000 K in these flowfields. Processes of interest include formation of negative ions and their subsequent fragmentation, excitation and deexcitation of long-lived excited electronic states, and electronic excitation of vibrationally excited molecules in their ground electronic states. The available data base of cross sections and rate coefficients for these electron-molecule collision processes is very fragmentary. This is particularly true for near-threshold excitation where the incident electrons have barely enough energy to drive the excitation. Furthermore, the experimental effort in the United States to determine these cross sections is very limited and shrinking.

Both measurements and calculations of low-energy electron-molecule collision cross sections are demanding. A strategy based on calculations of these cross sections and benchmark measurements for key species could be quite effective in meeting these needs. While the computational demands of these calculations have made such an approach impractical with conventional computers, large-scale parallel computers, with their orders-of-magnitude improvement over conventional computers, can greatly facilitate such a strategy. The objective of our work has been to exploit large parallel computers such as the Intel Paragon and CRAY T3D, with their hundreds of processors and gigabytes of memory, to calculate cross sections for electron-molecule collisions needed in modelling hypervelocity flows and plumes. The high profile and success of this effort have, in fact, enabled us to establish a collaboration with the leading experimental group in this field at Kaiserslautern University in Germany.

Accomplishments

At the relatively low impact energies of interest in these flows, an accurate quantum mechanical treatment of the full system, i.e., molecule plus electron, is essential to obtain reliable collision cross sections; low-order approximations are not applicable at these energies. In our studies of these collisions, we employ a multichannel extension of the variational principle originally introduced by Schwinger.[1] This multichannel variational principle was specifically designed to address low-energy electron-molecule collisions.[2] While the trial functions in this multichannel variational prinicple need not satisfy scattering boundary conditions,[1,2] matrix elements involving the free-particle Green's function which have no known analytic form arise and must be evaluated by quadrature. Evaluation of these matrix elements is the computational bottleneck in these calculations. In fact, the occurence of these matrix elements has been the greatest obstacle to the use of Schwinger-like variational principles, in spite of several desirable features of these approaches.

The two major tasks in the quadrature of these Green's function matrix elements are the evaluation and subsequent transformation of a large number ($\approx 10^{13}$) of electron repulsion integrals. These two tasks have been efficiently implemented on large-scale distributed-

memory parallel computers consisting of hundreds of microprocessors. While the overall performance of our parallel codes cannot be characterized by a single number, sustained performance of 5 to 10 GFLOP is typical.[3] To put this performance in perspective, our original sequential code averages about 0.03 GFLOP on a CRAY Y-MP processor. This increase in computational performance significantly enhances our ability to calculate the electron collision cross sections needed in modelling hypersonic flows and other weakly ionized plasmas.

Accomplishments during this period include:

• In a joint efffort with the experimental group of Professor H. Ehrhardt of Kaiserslautern University in Germany, we have completed a comprehensive study of the cross sections for electron impact excitation of the low-lying excited states of N_2 and CO from threshold to 3.7 eV above threshold. These studies should provide the most reliable estimates of these cross sections for N_2 and CO in the technically important, but experimentally challenging, near-threshold region. The availability of both differential and integral excitation cross sections offers significant opportunity for an in-depth comparison of the measured and calculated results. Cross sections have also been calculated for impact energies beyond the threshold region.

• Additional studies of cross sections for electron-NO collisions have been completed.

• We have published an invited article on these computational advances and applications in *Advances in Atomic, Molecular and Optical Physics* (Academic Press).

References

1. J. Schwinger, Phys. Rev. **72**, 742 (1947).

2. K. Takatsuka and V. McKoy, Phys. Rev. A **30**, 1734 (1984); C. Winstead and V. McKoy, Phys. Rev. A **47**, 1514 (1993).

3. C. Winstead, H. Pritchard, and V. McKoy, Computational Science and Engineering, Fall Issue, 34 (1995).

Publications resulting from research

1. Zobel, J., Mayer, U., Jung, K., Ehrhardt, H., Pritchard, H., Winstead, C., and McKoy, V., *Absolute Differential Cross Sections for Electron Impact Excitation of CO Near Threshold*, J. Phys. B **29**, 839 (1996).

2. de Paixão, F.J., Lima, M.A.P., and McKoy, V., *Elastic Electron-NO Collisions* , Phys. Rev. A **53**, 1407 (1996).

3. Winstead, C., and McKoy, V., *Highly Parallel Computational Techniques for Electron-Molecule Collisions*, Advances in Atomic, Molecular and Optical Physics, Edited by Bederson, B., and Walther, H. (Academic press, 1996).

4. Winstead, C., and McKoy, V., *Electron Scattering by Small Molecules*, Edited by Prigogine, I. and Rice, S.A. (Wiley Press, 1996).

5. Winstead, C., Pritchard, H., and McKoy, V., *Parallel Computation of Electron-Molecule Collisions*, Computational Science and Engineering, Fall Issue, **34** (1995).

Personnel Supported

Principal Investigator: Vincent McKoy, Professor of Theoretical Chemistry

Graduate Student: C-H. Lee

Research Fellow: C. Winstead,

Interactions/Transitions

1. Presentation: *High-Performance Simulation Tools for Microelectronics Fabrication*, Invited Talk at the Mardi Gras '96 Conference on Experimental and Simulation Challenges in Nano- Structured Materials, Baton Rouge, LA, February 1996.

2. Presentation:*Some Developments in Simulations of Plasma Reactors*, Invited Talk at the Center for Cooperative Research in Advanced Science and Technology, Nagoya University, Nagoya (Japan), December 1995.

3. Presentation: *The Impact of Parallel Computers: Electron Collision Data for Plasma Modelling*, National Plasma Data Center, Nagoya (Japan), December 1995.

4. Presentation*Studies of Electron-Molecule Collisions on Highly Parallel Computers*, Invited Talk at the Fourth Conference on Current Trends in Computational Chemistry, US Army Engineer Waterways Experiment Station, Vicksburg, MS, November, 1995.

5. Advisory: Member, Wright Laboratory Board of Visitors: Independent Strategic Assessment Group (Col. Richard Davis), 1996 -

Inventions: None.

Honors

B. V. McKoy: Fellow, American Physical Society, 1986 -

IV.3 NONEQUILIBRIUM LEEWARD SHOCK-VORTEX AERODYNAMICS

Objectives and Status of Research

The objectives of this research remain unchanged since the last report. In the past year progress has been made in further developing the new kinetic-based solver, called *EFMO* and

incorporating this scheme into our basic 3D Navier-Stokes solver *PGP3D* in such a way that it is part of a strongly coupled implicit treatment of the chemistry/ gas dynamics interaction. Further test calculations have been carried out on various flows including the interaction of an oblique shock wave with a boundary layer and very high resolution calculations of the frozen hypersonic flow past a cone at incidence. Similar calculations for hypervelocity cone-flow with equilibrium chemistry and with finite-rate chemistry are currently being attempted.

IV.3.1 Tests of EFMO scheme for frozen flow.

The *EFMO* scheme was described in detail in the last report. Briefly, this is a kinetic-based flux-split method modified to reduce its numerical viscosity using modified Osher intermediate states. EFMO can withstand extreme conditions ranging from near vacuum to very intense shock waves and rarefaction waves where many regular flux-difference schemes fail in the absence of ad hoc fixes. The details of this method together with a set of tests on unsteady one-dimensional, and two-dimensional inviscid and viscous supersonic and hypersonic flows have been published (Moschetta & Pullin 1996a). We show two relevant test results, both for frozen flow. The first is a 2D viscous flow which consists of the interaction of an oblique shock wave with a laminar boundary layer.

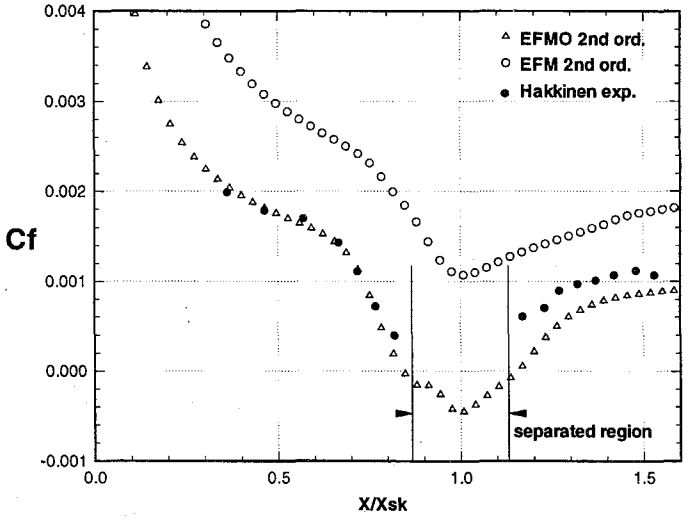

Figure IV.4. Shock-boundary layer interaction. Comparisons of $Cf = \tau/(\rho_\infty u_\infty^2/2)$ with the experimental results of Hakkinen et al. (1959). Conditions are $M_\infty = 2.0$, $Re_\infty = 2.96 \times 10^5$ based on the distance the leading edge to the interaction point. The incident shock wave is imposed such that the shock intersects the flat plate at 32.6^o.

The impinging oblique shock incident upon the boundary layer on the flat plate is chosen to be strong enough to cause the boundary layer to separate from the surface and reattach downstream. The computational results were obtained using a 50×50 grid above the plate surface spaced such that approximately 15 points spanned the boundary layer. In Fig. IV.4

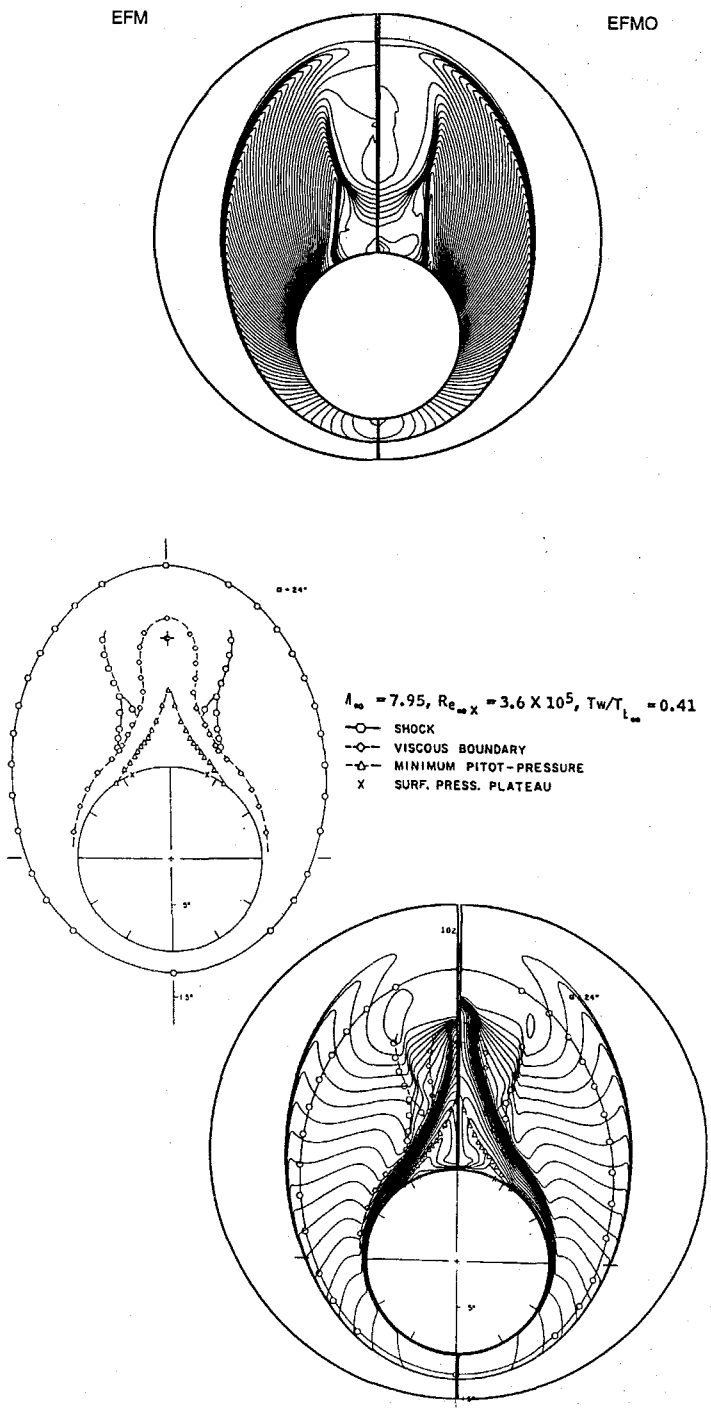

Figure IV.5. Flow property profiles on a cone of half-angle 10^0 at zero incidence in a hypersonic stream at $M = 7.95$. Frozen flow, $R_e = 4.2 \times 10^5$ based on distance L from apex and $Pr = 1$. $T_w/T_\infty = 0.41$. Stepback calculation with 250×300 cells in the cross section. Top ; $\log(p/p_\infty)$. Bottom; superposition of Mach number contours with total head results of Tracy (1963), also shown as inset. In each contour plot the right side shows the *EFMO* and the left side the *EFM* calculation.

calculations of the skin friction $C_f = \tau/(\rho_\infty u_\infty^2/2)$ are compared with the experimental results of Hakkinen et al. (1959). Conditions are $M_\infty = 2.0$, $Re_\infty = 2.96 \times 10^5$ based on the distance the leading edge to the interaction point. The incident shock wave is imposed such that the shock intersects the flat plate at 32.6°. Note that the experimental probes in the separated region were unable to measure skin friction other than to show that it was zero or negative. The numerical results obtained with EFMO are very consistent with experimental data. The skin friction of the EFMO scheme behind the separation region is lower than that of experiment, which is also predicted by other computational results.

The second test shows frozen flow past a cone of half-angle 10^o at 20^o incidence in a hypersonic flow at $M_\infty = 7.95$ chosen to match the experimental conditions used by Tracy (1963). The Prandtl-number was $Pr = 1$ and a wall temperature $T_w/T_\infty = 0.41$ was used. Fig. IV.5 shows flow properties at a distance L at which $R_e = 4.2 \times 10^5$ based on L and free-stream conditions. The calculations were done in high resolution on the Caltech *Delta* parallel machine using the so-called "step-back" method, in which the flow is assumed to be locally conical over several cells in the axial direction whose axial cell dimension is small compared to the distance of the cell centroids from the cone apex. This is an approximation. The results of this calculation using 250 × 300 cells in the cross-section orthogonal to the cone axis are shown in Fig. IV.5. The *EFMO* calculation can be seen to capture the location of the position of the cross-flow shock and and the separated shear layer, but the bow shock lies further from the body in the calculations. This may be a result of the locally conical approximation. We remark that the main idea of the step-back/conical approximation is to provide upstream boundary conditions for more refined calculations than are displayed in Fig. IV.5.

IV.3.2 EFMO and IDG Chemistry

Two versions of *PGP3D* incorporating the Lighthill-Freeman ideal-dissociating gas (IDG) chemistry model were discussed in the last report. The first of these (*PGP3D.3*) is based on an operator-splitting approach whilst in the second approach, the implicit *PGP3D/EFMO* is extended to include IDG chemistry in a partially implicit way (*PGP3D.4*; Jean-Marc Moshetta). Both of these schemes have been applied to the cone flow with equilibrium and with finite-rate chemistry using a semi-marching technique. In this method, the stepback technique is first applied to the flow at a station very near the apex; the calculation then proceeds to "march" downstream by solving the full (non-parabolized) unsteady equations sequentially on a series of overlapping grids along the cone axis. The calculation is started using the step-back method. Each grid is 3-10 cells long in the axial direction and the overlap between successive grids is 1-3 cells. This method works extremely well for chemically active inviscid flow, and has been extensively tested for these flows.

However problems have been encountered for viscous flow when (*PGP3D.3*) is used, owing to the very slow convergence rate of the explicit method. This semi-marching method is currently being tested for frozen flow and for chemically equilibrium flow using the implicit solver(*PGP3D.4*) with mixed results. It is possible that it will fail to give a globally convergent solution for viscous flow owing to the presence of a thin elliptic region of the flow in the subsonic part of the boundary layer. If this is the case, we will need to revert to a global

implicit Navier-Stokes calculation, using a step-back calculation applied at low Reynolds number near the cone apex, to provide upstream boundary conditions in the region between the bow shock wave and the cone surface. This can be done at the cost of lower resolution in planes (or spherical surfaces) orthogonal to rays from the cone apex.

References

R. J. Hakkinen, I. Greber, L. Trilling, S.S. Abarbanel, *NASA Memo 2-18-59W*, 1959 .

Tracy, R.R., 1963 Hypersonic Flow Over a Yawed Circular Cone, Hypersonic Research Project Memorandum No. 69, Graduate Aeronautical Laboratories, California Institute of Technology, Pasadena, California

Publications Resulting from Research, 1995-96

Mallett, E.R. Pullin, D.I. and Macrossan, M.N., "A numerical study of hypersonic leeward flow over a blunt nosed delta wing". *AIAA J.* **33**, 1626-1633, 1995.

Moschetta, J-M. & Pullin, D.I, "Computation of hypersonic viscous flows: are robustness and accuracy compatible?", AIAA paper 96-2087. Preseented at 27th AIAA Fluid Dynamics Conference, New Orleans, 1996a.

Moschetta, J-M. & Pullin, D.I, "A robust low diffusive kinetic schme for thr Navier-Stokes/Euler Equations". Subjudice *J.Comp. Phys.* 1996b.

Personnel Supported

1. D. Pullin, Professor of Aeronautics
2. Shaun Shariff, Postgraduate student.

Interactions/Transitions

(a) Participations/presentations at meetings etc.

Moschetta, J-M. & Pullin, D.I, "Computation of hypersonic viscous flows: are robustness and accuracy compatible?"Presented at 27th AIAA Fluid Dynamics Conference, New Orleans, June 1996.

(b) Consultative and advisory functions: None

(c) Transitions: None

New discoveries: None

Honors/Awards: None

Chapter V: DIAGNOSTICS

V.1 DIAGNOSTICS WITH LASER-INDUCED THERMAL ACOUSTICS

Accomplishments, New Findings.

In order to assess the viability of LITA at the temperatures that are experienced in T5, a series of experiments were conducted using a closed shock tube with a combustion-heated driver gas. LITA measurements were taken in the reflected shock region near the end wall of the shock tube. Figure V.1 is a schematic diagram of the experimental apparatus in these studies. This apparatus can generate temperatures well in excess of 5000 K in air at the densities that are required for LITA, *i. e.*, mean-free paths less than the grating wavelength.

The results of the all the tests are summarized in Table V.1. Pressure transducers in the shock tube provided incident shock speeds and pressure information. Using this information, the STANJAN chemical equilibrium computer code provided estimates of the reflected-shock-region conditions. The estimated sound speeds compare well with the LITA measured values (generally within 10%). In exceptional cases with worse agreement, the signals were ill-conditioned for sound-speed measurement and the combined effects of turbulence in the sample volume and noise complicated the (automated) procedure of fitting the theoretical and experimental signals. The conclusions that were drawn from these experiments were that the degree of disagreement between the estimated and measured signals was within the uncertainty of the estimates. The next series of these experiments will employ a special triggering device (LabSmith LC884) which can dynamically measure the incident shock speed and time the firing of the laser with high accuracy. This improvement will reduce the composition uncertainty and turbulence levels in the measurement sample.

During the past year, LITA experiments also progressed on other fronts. Single-shot signal histograms were recorded to establish the repeatability of LITA measurements at different levels of signal to noise ratio. Figure V.2 is a histogram of LITA sound speed measurements taken with an apparent signal to noise ratio of 5 (Cummings et al., 1996a). The inset signal is typical of the series that produced the histogram. The RMS deviation about the mean sound-speed measurement is less than 0.3%. This performance figure improves dramatically with signal to noise ratio, provided that the beams are aligned accurately.

In addition, the first heterodyne LITA velocimetry measurements were demonstrated (Cummings et al., 1996b). These measurements were taken at elevated pressures and room temperature in the high-pressure cell with a stirring fan that was used to generate turbulence. The velocity measurements agree reasonably well with estimates that are based simply on a balance of turbulent kinetic energy addition (via the fan) and viscous dissipation (Cummings 1995). The velocity measurements also agree with the results of a study of the effects of fan

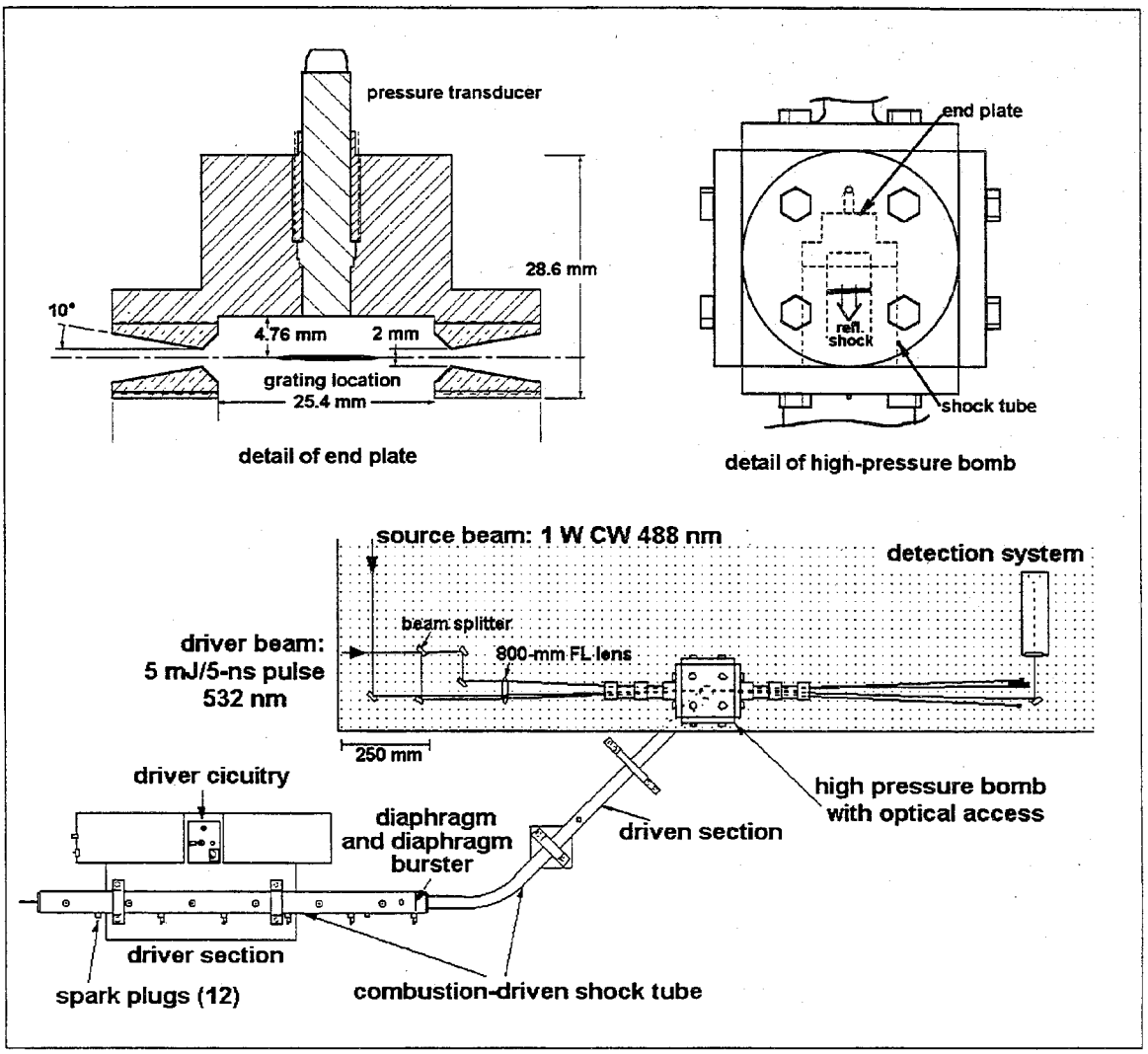

Figure V.1. Schematic diagram of the combustion-driven shock tube experiments. The driver gas is a mixture of helium (79%), hydrogen (14%) and oxygen (7%). The test begins by firing twelve spark plugs simultaneously in the driver tube, igniting the gas mixture. When the driver-gas pressure peaks (20 ms after firing) the shock-tube diaphragm is burst via an electrical discharge. The driven tube has a 45° and a 90° bend, followed by a straight vertical section approximately 500-mm long. The incident shock wave travels through the tube and into a high-pressure bomb with optical access. The shock reflects off an end plate and a LITA signal is measured through 2-mm diameter optical ports.

Test ID	Sound speed estimated by STANJAN m/s	Sound speed measured by LITA m/s	Percent difference
T0222A	713	711 0	.3
T0221B	740	713	3.7
T0401A	750	863	−13.
T0327D	760	574	24.
T0401B	779	804	−3.2
T0306D	790	712	9.9
T0402A	791	886	−11.
T0327A	794	696	12.
T0402B	814	814	0.07
T0326A	832	976	−14.
T0320B	837	897	−6.7
T0402C	896	873	2.7
T0402D	897	1020	−12.
T0320C	911	910	0.1
T0402E	948	1000	−5.7
T0321B	973	988	−1.5
T0222C	1000	1130	−11.
T0405B	1035	1126	−8.0
T0405A	1037	1067	−2.8
T0405C	1107	1118	−0.9
T0411C	1116	1235	−9.6
T0408B	1143	941	17.
T0408D	1153	1081	6.2
T0411B	1179	1178	0.06
T0409A	1214	1253	−3.1
T0409B	1254	1311	−4.4
T0410C	1340	1373	−2.4

Table V.1. SUMMARY OF THE LITA SOUND SPEED MEASUREMENTS. Sound speed estimates were based on measured incident shock speeds and pressures and made using STANJAN, a chemical equilibrium computer program. The LITA measurements are obtained via FitLITA an automated/interactive nonlinear fitting program for LITA signals that was developed for this project.

turbulence on homodyne LITA signals.

Our tests show that turbulence effects on LITA signals are rational, but complicated, and can degrade LITA measurement accuracy and precision. The destruction of induced gratings by small-scale turbulence enhances diffusion, thus LITA measurements over-predict diffusivities when turbulence is present. Turbulence at length scales near that of the induced grating can cause large deviations from theoretical signal shapes, raising the uncertainty of parameters measured by a best fit to theory. The magnitudes of these effects depend upon beam geometrical parameters, the fluctuation Reynolds number, and the Knudsen number. For a

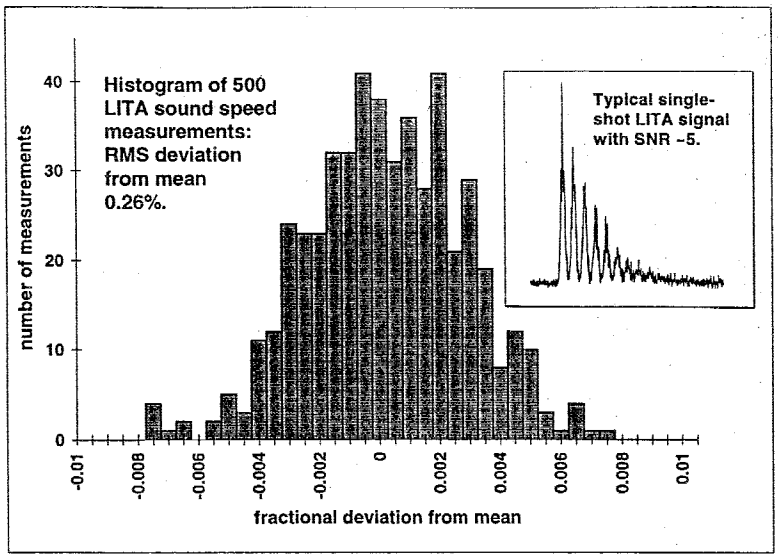

Figure V.2. Histogram of 500 independent, single-shot LITA measurements on a sample of NO_2-seeded air at room temperature and atmospheric pressure. The inset signal typifies those that produced this histogram, with an apparent signal to noise ratio of 5. The RMS deviation in measurements is less than 0.3%. This deviation decreases dramatically with improved signal purity.

quick estimate of the importance of turbulence effects, the relevant Kolmogorov time scale of the flow may be compared to the diffusion-limited grating lifetime. The measured grating lifetimes always follow the shorter of the two times, evidenced by experiments on fan turbulence (fluctuation speeds of ¡3 m/s) and shock-tube flows (fluctuation speeds up to 300 m/s). This study will continue since turbulence affects our combustion-driven shock tunnel measurements and will be important in other applications of LITA.

Personnel Supported

1. Hans G. Hornung, Kelly Johnson Professor of Aeronautics, GALCIT Director.
2. Eric B. Cummings, Staff Scientist
3. Bonifacio Calayag, Graduate Research Assistant
4. Geoffrey Mach, Senior Student
5. Bahram Valiferdowsi, Associate Engineer

Publications Resulting from the Research

Cummings E. B., Hornung H. G., and Brown M. S., 1996, Laser-induced thermal acoustics (LITA)
measurement of gas properties in *Shock Waves*, Proc. 20th Symp. on Shock Waves, World Scientific, Singapore.

Cummings E. B., Brown M. S., Calayag B., Hornung, H. G., 1996a, Laser-induced thermal acoustics (LITA) measurements
at high temperature and pressure, *Opt. Lett.*, in preparation.

Cummings E. B., Brown M. S., Calayag B., Hornung, H. G., 1996b, Effects of flow and turbulence on Laser-induced
thermal acoustics (LITA) signals, *Applied Optics*, in preparation.

Interactions/Transitions

1. Presentation of seminar at United Technologies Research Center, East Hartford, CT, May, 1996 (Cummings).
2. Presentation of seminar at DLR Göttingen, Germany, June, 1996 (Cummings).
3. Presentation of poster at Gordon Conference on Laser Diagnostics in Combustion, Plymouth, NH, July, 1996 (Cummings).
4. Presentation of seminar at Princeton University, September 19, 1995 (Cummings)
5. Attendance at Workshop on Radiatively Driven Hypersonic Wind Tunnel Concept, Wright Labs, Dayton, April 25-26, 1996 (Hornung).
6. Attendance and presentation at Workshop on Plasma-Based Hypersonic Drag Reduction, Major Scott Schreck, Wright Labs, May 10, 1996 (Hornung).
7. Presentation of seminar at the Scripps Institution of Oceanography, May 16, 1996 (Cummings)
8. Presentation of nominated talk at session on Experimental Methods in Fluid Mechanics, International Congress of Theoretical and Applied Mechanics, Kyoto, August 25-31, 1996 (Hornung and Cummings)
9. Transfer of LITA technology to MetroLaser personnel (M. Brown) in preparation for their NASA funded research.

Honors/Awards

Milton and Francis Clauser Prize for Caltech Ph. D. Thesis: E. B. Cummings, 1995

Ballhaus Prize for GALCIT Ph. D. Thesis: E. B. Cummings, 1995, shared.